J. Anat. (2002) **200**, pp377–390

REVIEW

Comparison of a new pmp22 transgenic mouse line with other mouse models and human patients with CMT1A*

A. M. Robertson,[1,2] J. Perea,[1,5] A. McGuigan,[1,6] R. H. M. King,[2] J. R. Muddle,[2] A. A. Gabreëls-Festen,[4] P. K. Thomas[3] and C. Huxley[1]

[1]*Division of Biomedical Sciences, and Clinical Sciences Centre, Imperial College School of Science, Technology and Medicine, Hammmersmith Hospital Campus, London, UK*
[2]*University Department of Clinical Neurosciences, Royal Free & University College Medical School, London, UK*
[3]*University Department of Clinical Neurology, Institute of Neurology, London, UK*
[4]*University Hospital Nijmegen, Department of Neurology, Nijmegen, the Netherlands*

Abstract

Charcot-Marie-Tooth disease type 1A is a dominantly inherited demyelinating disorder of the peripheral nervous system. It is most frequently caused by overexpression of peripheral myelin protein 22 (PMP22), but is also caused by point mutations in the *PMP22* gene. We describe a new transgenic mouse model (My41) carrying the mouse, rather than the human, *pmp22* gene. The My41 strain has a severe phenotype consisting of unstable gait and weakness of the hind limbs that becomes obvious during the first 3 weeks of life. My41 mice have a shortened life span and breed poorly. Pathologically, My41 mice have a demyelinating peripheral neuropathy in which 75% of axons do not have a measurable amount of myelin. We compare the peripheral nerve pathology seen in My41 mice, which carry the mouse *pmp22* gene, with previously described transgenic mice over-expressing the human PMP22 protein and Trembler-^{J} (Tr^{J}) mice which have a P16L substitution. We also look at the differences between CMT1A duplication patients, patients with the P16L mutation and their appropriate mouse models.

Key words myelin; neuropathy; PMP22; Trembler-J mouse.

Introduction

Charcot-Marie-Tooth disease type 1A is a dominantly inherited demyelinating disorder of the peripheral nervous system. It is most frequently caused by over-expression of the *PMP22* gene due to duplication of a 1.5-Mb region on chromosome 17 but it can also result from point mutations in the *PMP22* gene (Lupski et al. 1991; Raeymaekers et al. 1991; Pentao et al. 1992; Wise et al. 1993; Nelis et al. 1996; Reilly, 1998).

Over the past few years several pmp22 over-expressing animal models have demonstrated a dose dependent response of peripheral nerve myelination to increased pmp22 levels (Magyar et al. 1996; Sereda et al. 1996; Huxley et al. 1998). tgN248 mice with a high copy number (16) of the mouse *pmp22* gene completely fail to elaborate myelin (Magyar et al. 1996). Mice with lower copy numbers of the human gene demonstrate developmental delays in myelination, decreased numbers of myelinated fibres and abnormally thin myelin (C22 with seven copies) or normal development and subsequent demyelination of a population of larger fibres (C61 with four copies) (Huxley et al. 1998).

There are five amino acid differences between the mouse and rat proteins, 22 between the human and rat and 22 between the human and mouse. As it is not known what aspect of protein structure causes the

Correspondence
Dr C. Huxley, Division of Biomedical Sciences, and Clinical Sciences Centre, Imperial College School of Science, Technology and Medicine, Hammmersmith Hospital Campus, London W12 ONN, UK.
E-mail: c.huxley@ic.ac.uk
Present addresses: [5]*Genethon III, Evry Cedex, France*; [6]*Biological Services Unit, King's College, London, UK.*
**From a paper presented at a one-day symposium on Peripheral Nerve and Neuropathies, to celebrate the contribution of P. K. Thomas as Editor of the Journal of Anatomy, 1990–2001, at the Institute of Neurology, Queen Square, London, UK, 22 March 2002.*

Accepted for publication *14 February 2002*

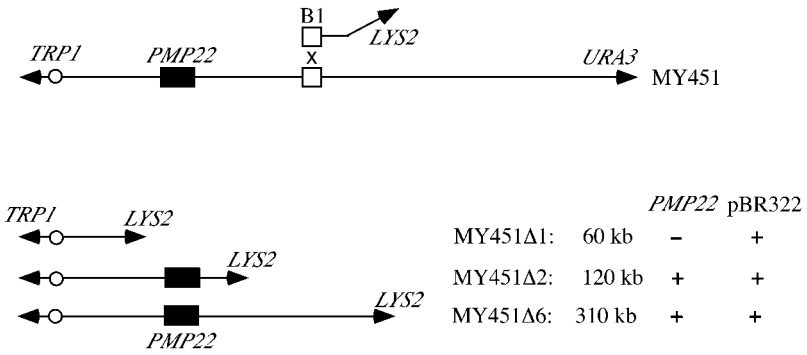

Fig. 1 Truncation of the 800-kb YAC MY451 to generate the 310-kb YAC MY451Δ6 which was used for microinjection.

dominant phenotype in human patients with point mutations, it is possible that PMP22 from another species will actually cause a dominant negative effect on the phenotype rather than an over-expression phenotype. To test whether the phenotypes in our mouse models with the human gene (C22 and C61) are truly due to over-expression, we have now made a transgenic mouse line with the mouse *pmp22* gene.

Transgenic mice are widely used as models of human disease and are a valuable tool for elucidating the mechanisms of disease and in developing therapies. The pathology resulting from the same mutation may, however, vary between mice and men. Here we examine the differences in the response of human and murine peripheral nervous systems to over-expression and to the P16L mutation. The PMP22 over-expressing animal models C22 and My41 show similar deficits in myelination but the pathology is different both qualitatively and quantitatively from that seen in over-expressing humans. Likewise, the PMP22 point mutation P16L, which has occurred spontaneously in both humans and mice, results in pathology that is markedly different in mice compared to humans (Gabreëls-Festen et al. 1995; Robertson et al. 1997).

Materials and methods

Pmp22 YAC

Various mouse genomic YAC libraries were screened by the Genethon Mouse YAC Screening Service by PCR with the following mouse *pmp22* exon 4 primers: 5′CGGCCGCCTTTGGTGAGA and 5′AATGGCTGCAGTCTGTCC. An 800-kb clone, MY451 (also called M4F12), from the MIT library (Haldi et al. 1996) was chosen for further work. This library is derived from C57BL/6 J DNA and is constructed in the pRML1 and pRML2 vectors.

It is very difficult to purify an 800-kb YAC intact for micro-injection, so the YAC was truncated by homologous recombination in yeast with the pB1F vector. This vector is a derivative of pBCL8.1 (Lewis et al. 1992) constructed by J. C. Edmonson and R. Rothstein. It contains a B1 mouse repetitive SINE element (in place of the human Alu element present in pBCL8.1), an *LYS2* gene to allow selection of recombinant yeast clones and a telomere to stabilize the truncated YACs. After vector linearization and yeast transformation, the clones in which a recombination event has occurred between the plasmid and a B1 element in the YAC can be recognized by their Lys + Trp + Ura– phenotype (Fig. 1). The MYF451 yeast strain was transformed with 3 μg of *Sal*I linearized pB1F DNA. We obtained a collection of truncated YACs ranging from 60 to 730 kb. This allowed the *pmp22* gene to be located between 60 and 120 kb from the centromeric end of the YAC. A 310-kb derivative, MYF451Δ6, with at least 60 kb and 90 kb flanking the *pmp22* gene on either side, was chosen for micro-injection (Fig. 1).

Generation of transgenic mice

YAC DNA was isolated from preparative pulsed field gels using a modification of a previously described method (Gnirke et al. 1993). After treatment with agarase the DNA solution was concentrated about two-fold with a Millipore Ultrafree-MC 30 000 NMWL Filter Unit (Millipore Cat # UFC3 TTK 00) and then dialysed for several hours on a Millipore filter (cat no. VMW 02500, type VM, pore size 0.05 μm) against micro-injection buffer (10 mM Tris pH 7.4, 0.2 mM EDTA, 100 mM NaCl). Transgenic mice were generated by standard techniques of pronuclear injection (Hogan et al. 1986) using C57BL/6J × CBA/Ca F2 oocytes. Subsequent crosses were to C57BL/6J × CBA/Ca F1 mice. All

work with mice was carried out under appropriate Home Office Licences.

Histology

Nerve samples from transgenic mice were processed for light and electron microscopy. Tissues were fixed in 1% glutaraldehyde and 1% paraformaldehyde in 0.1 M PIPES buffer, post-fixed in 1% osmium tetroxide, dehydrated through increasing concentrations of ethanol and embedded in Durcupan via 1,2 epoxy propane. Thin sections for light microscopy were stained with thionin and acridine orange and ultrathin sections were contrasted with uranyl acetate and lead citrate.

Animals used for morphological studies were up to 18 months of age with the exception of My41 mice which were killed at 4–6 months of age.

Morphometry

Fibre counts and measurements were performed using a Zeiss Axioplan with a Martzhauser motor-driven stage connected to a Zeiss KS400 image analysis system (Image Associates, Thame, UK).

Measurements of myelin periodicity were performed on TV images from a Zeiss 902 Electron microscope using AnalySIS software to measure 20 lamellae in 20 myelin sheaths on each section examined.

Counts of promyelinated fibres, Schwann cell nuclei and axons incompletely surrounded by Schwann cell cytoplasm were carried out on non-overlapping electron microscope fields at a magnification of 7000×. A total area of 0.63 mm^2 was analysed from the sciatic nerves of p4 and p10–12 mice. Promyelin fibres were defined as those axons that had separated from axon bundles and were associated with a single Schwann cell.

Statistical analysis used Unistat software to calculate significance using the Mann–Whitney non-parametric test. Error bars indicate standard deviations.

Results

Description of the My41 mouse line

A 310-kb YAC 'MYF451Δ6' carrying the mouse *pmp22* gene with at least 60 kb and 90 kb of flanking DNA was isolated as described in Materials and methods. Three lines of transgenic mice were generated with this YAC (JΔ42, My39 and My41), all of which carried the left and right arms of the YAC. Of these, JΔ42 and My39 had no detectable histological myelin abnormality even when homozygous, suggesting that the *pmp22* region of the YAC may not have been transferred. As the YAC contains mouse genomic DNA and there are always two normal copies of the mouse *pmp22* gene it is technically difficult to determine whether the central region of the YAC has been transferred intact and no attempt was made to verify this.

The My41 founder mouse was a chimeric male who appeared normal, bred well and transmitted the transgene to less than 10% of his offspring. The completely transgenic mice of subsequent generations had a very severe phenotype consisting of unstable gait and weakness of the hind limbs. Gait abnormalities in My41 mice became obvious by 3 weeks and progressively worsened. Most mice had to be killed between 4 and 5 months of age due to general weakness and disability. Female My41 mice had one, or at most two, litters when mated with wild-type males, but then ceased to reproduce. The males did not breed with wild-type females. The levels of *pmp22* RNA were not determined as the very severe demyelination is likely to result in relatively low levels of total RNA. DNA copy number was not determined.

Pathology of My41 mice

My41 mice have a severe demyelinating peripheral neuropathy (Fig. 2D) with no evidence of hypertrophic changes (increased fascicle size) or of classical onion bulbs. The majority of axons (73.7%) have either no myelin at all or myelin that is too thin to be measured at the light microscope level (fewer than five lamellae) (Fig. 3). We have termed these fibres 'dysmyelinated' as their axons are of sufficient diameter that one would normally expect them to be myelinated. Dysmyelinated fibres represent fibres that have either been demyelinated or have completely failed to elaborate any myelin. The fibre size distribution shows a lack of large myelinated fibres and the appearance of a population of dysmyelinated fibres (Fig. 4). As would be expected for such a high degree of dysmyelination, the number of Schwann cells was increased in My41 mice (Fig. 3). There were approximately three times the normal number of Schwann cells.

Where myelin sheaths were present in My41 mice, they had an increased g ratio (Fig. 3). As myelin sheath thickness is normally a function of axon size, g ratios

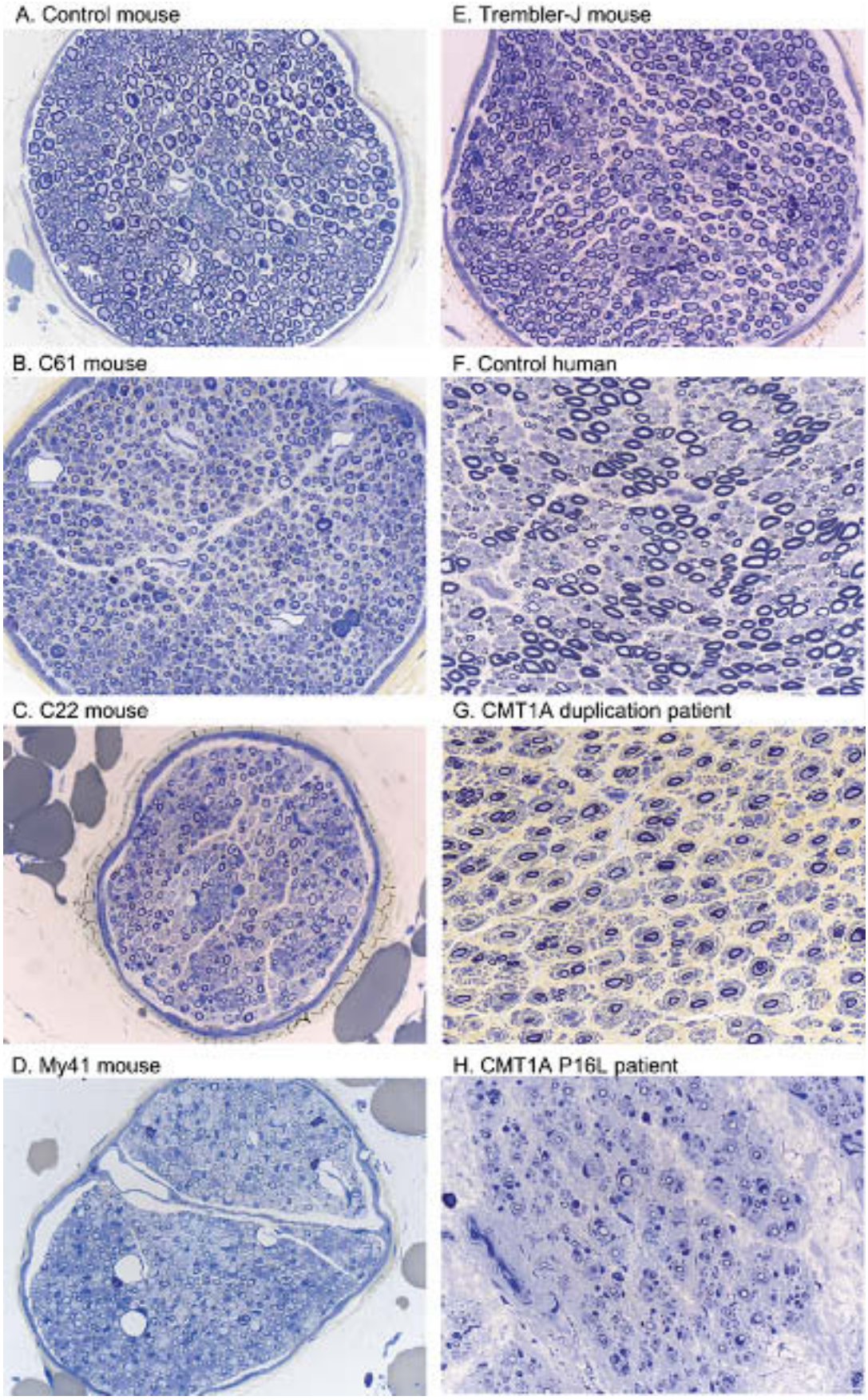

Fig. 2 Histological sections. A,B,C,E: tibial nerves from 18-month-old mice. D: tibial nerve from 5-month-old mouse. F–H: sural nerves from patients.

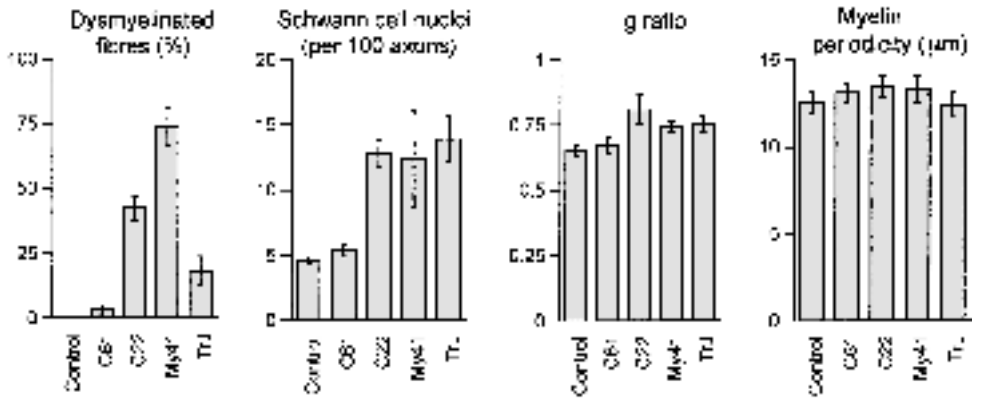

Fig. 3 Histograms of histological features in control, C61, C22, My41 and Tr^{J} mice. Dysmyelinated fibres are given as the proportion of the total number of singly ensheathed fibres for six mice from each strain. Schwann cell nuclei are given as number counted per 100 axons from sciatic nerve for groups of six mice from each strain. g ratio is the ratio of axon diameter/fibre diameter for myelinated fibres from groups of six mice. Myelin periodicity (μm) was calculated for 20 fibres from each of six mice. Control, C61, C22 and Tr^{J} mice (all 7–9 months), My41 mice (5 months old).

provide a measure of relative myelin thickness (axon diameter/fibre diameter) avoiding any bias due to altered fibre size distributions. The g ratio of 0.74 in My41 mice vs. 0.65 in control mice indicates that the myelin is markedly thinner in My41 than normal mice. The myelin periodicity was slightly but not significantly increased compared with control mice (Fig. 3).

In normal mice, bundles of small unmyelinated axons are associated with one Schwann cell to form what are known as Remak fibres (Fig. 5A). These can be distinguished from promyelinated fibres in an arrested stage of development as there are multiple axons surrounded by a single Schwann cell. In the My41 mice these unmyelinated axons show an excess of Schwann cell membrane formation similar to those shown in C22 animals (Fig. 5B).

There was no evidence of axon loss at the mid sciatic level in 5-month-old My41 mice (Fig. 6) but axonal loss was identified by the presence of bands of Büngner and empty basal laminal tubes in both the proximal and the distal tibial nerves of 5–6-month-old My41 mice.

Cross-sections of sciatic nerve from animals at postnatal day 4 (P4) and days 10–12 (P10–12) were examined by electron microscopy to analyse the development of demyelination. At P4, myelination was already delayed in My41 mice with the proportion of myelinated axons being only 4.6% compared to 54.2% in control animals (Fig. 7). The proportion of myelinated axons had increased to 14% by P10–12 but this is still less than 20% of control values. The level of myelination increased slightly with age, and approximately 25% of axons were myelinated in adult mice. Many dysmyelinated axons were incompletely surrounded by Schwann cell cytoplasm, and others did not have any visible Schwann cell contact (Fig. 8A).

Pathology of human PMP22 transgenic mice

The histology of the transgenic lines C22 and C61 that carry the human *PMP22* gene was also analysed. Histograms of fibre size distributions show a decrease in the proportion of large myelinated fibres and an increase in the proportion of smaller ones (Figs 3 and 4). The percentage of dysmyelinated fibres is only 3.1% in C61 compared to 42.4% in C22, reflecting the lower expression of PMP22.

The Schwann cell number is increased in the C22 mice as previously described (Robertson et al. 1999) (Fig. 3). The g ratio is significantly increased, indicating inappropriately thin myelin sheaths (Fig. 3). Neither of these aspects are affected in the mildly affected C61 strain.

The lack of coverage of the axolemma by the Schwann cells, previously reported in Tr^{J} mice (Robertson et al. 1997), was also characteristic of C22 mice (Fig. 8A). The relationship of Schwann cell to axon appeared normal in the C61 mouse nerves.

Measurement of myelin periodicity showed a significant increase in the C22 mouse nerves (Fig. 3) whereas the C61 myelin was normal. Uncompacted myelin was also only seen in C22 mouse nerves and was not found in the C61 mice. C61 mice did not show the ultrastructural signs of fibre degeneration that were seen in the C22 mice. The abnormal Remak fibres seen in the

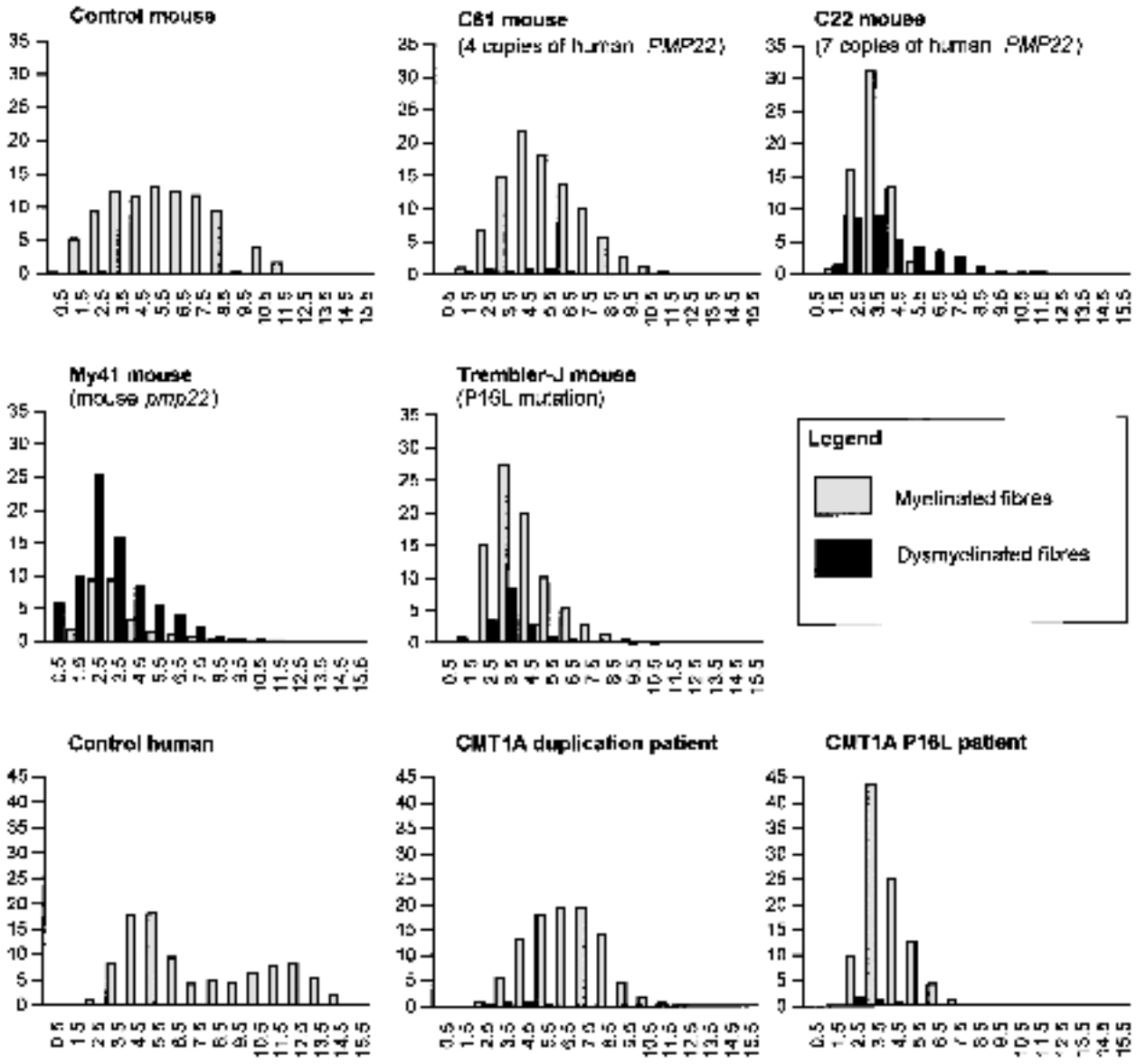

Fig. 4 Fibre size distributions (μm) taken from the sciatic nerves of groups (n = 6) of Control, C61, C22 and Tr^J mice (all 7–9 months old), and My41 mice (5 months old) and the sural nerve of representative control, CMT1A duplication and P16L patients. The percentage of myelinated or dysmyelinated fibres in each size range is indicated.

My41 mice were also seen in the highly over-expressing duplication model C22 (Fig. 5B) but not in the mildly affected C61 strain.

Classical onion bulbs were rarely seen in any of the strains examined in this study; however, they were found in the tibial nerve of an 18-month control mouse at the ankle (Fig. 9A).

Pathology of Trembler-J mice

Histological analysis showed that 18.4% of fibres were dysmyelinated in Tr^J mice and the relationship with Schwann cells has already been reported as abnormal (Robertson et al. 1997). The Schwann cell number is increased as previously described (Robertson et al. 1999) (Fig. 3). The g ratio is significantly increased, indicating inappropriately thin myelin sheaths (Fig. 3) but myelin periodicity was found to be the same as in normal mice (Fig. 3).

The incidence of ultrastructural signs of axonal degeneration at 8 months appeared similar to that seen in My41 and C22 mice; however, fibre counts in the sciatic nerve at 8 months did not differ from normal (Fig. 6). The unmyelinated fibre bundles of Tr^J animals

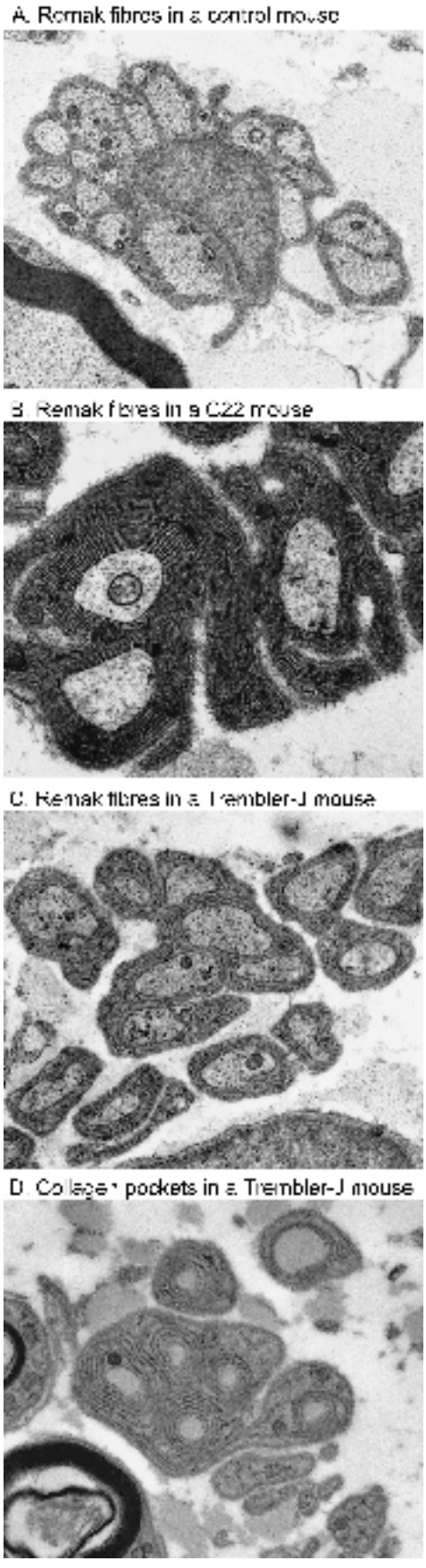

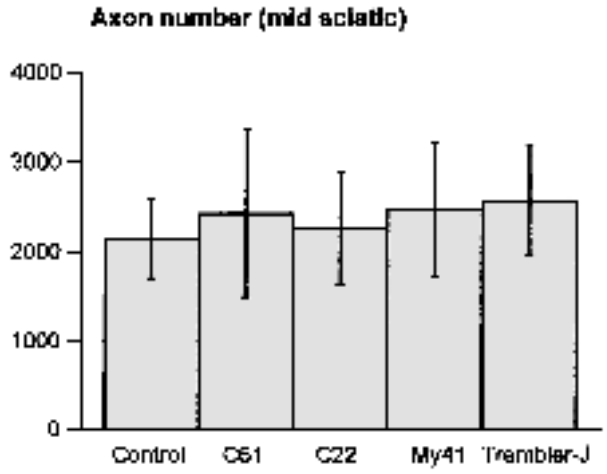

Fig. 6 Number of axons present in the mid sciatic nerves of 7–9-month-old animals (six of each strain), except My41 which were 5 months old (n = 6). Axons with a diameter greater than 1 μm were counted.

show less excess membrane formation than the over-expressing models but similar structures were also found around bundles of collagen fibrils (collagen pockets), suggesting a Schwann cell recognition problem (Fig. 5C,D).

Discussion

Comparison of over-expressing and mutant PMP22 mouse strains

The My41 mice carry extra copies of the mouse *pmp22* gene, the C61 and C22 mice carry four and seven copies, respectively, of the human *PMP22* gene, while Tr^J mice have the P16L missense mutation. The histology of these lines was compared to determine whether there were any qualitative differences that could be due to over-expression of the mouse protein compared with over-expression of the human protein or the dominant negative effect of the P16L mutation. My41 mice represent a true over-expression model compared with C22 and C61 in which the human protein could have a dominant negative or over-expression effect.

Pathologically, demyelination is the dominant feature of all the PMP22 mutant mice we examined. All the mutant mouse strains examined (Trembler –

Fig. 5 Unmyelinated fibre bundles. A: Remak fibres in a control mouse. B: extensive Schwann cell layers wrapping around Remak fibres in a C22 mouse. C: Schwann cell layers around Remak fibres in a Tr^J mouse. D: layers of Schwann cell membrane seen around collagen pockets in a Tr^J mouse.

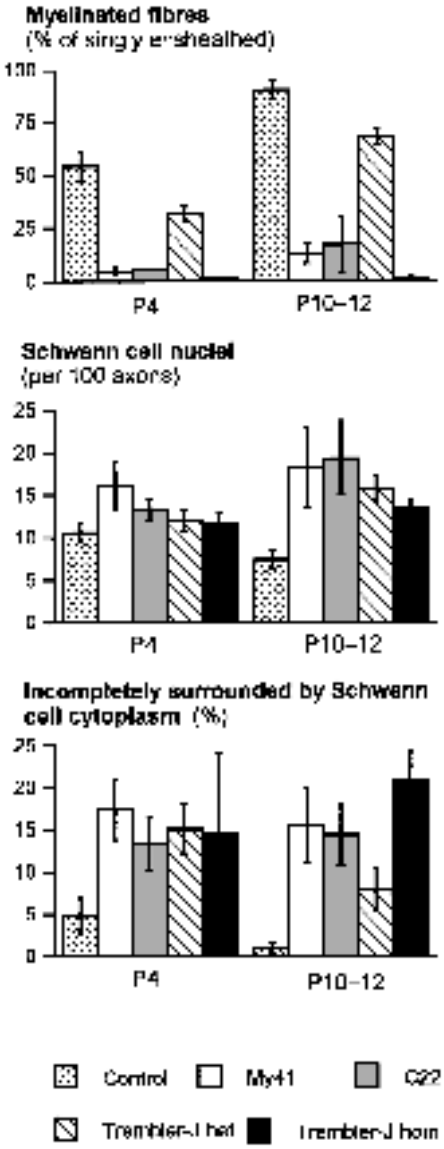

Fig. 7 The development of myelination abnormalities in early postnatal mice. Graphs show the percentage of myelinated fibres, Schwann cell nuclei per 100 axons and the percentage of axons incompletely surrounded by Schwann cell cytoplasm. In each case, groups of seven mice (four in the case of My41) were counted. Animals were analysed at postnatal days 4 (P4) and postnatal days 10–12 (P10–12) as indicated.

data not shown, Tr^J, C61, C22 and My41) had a distinct population of dysmyelinated axons that are without detectable myelin but whose diameters are of a size that should normally be myelinated. The percentage of affected fibres varied from 3.1% in C61 to 73.7% in My41. It is probable that these dysmyelinated fibres represent a generalized reaction of the murine peripheral nervous system to disorders of myelination as they are also seen in other mouse models that

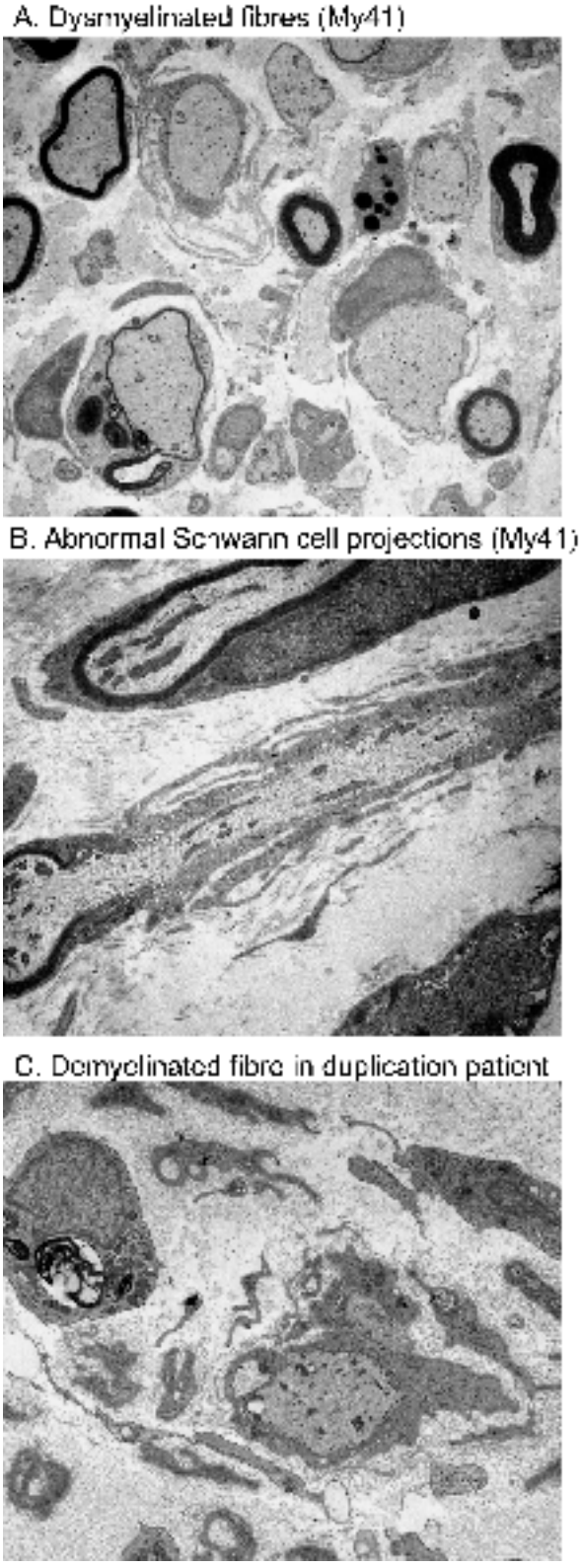

Fig. 8 Schwann cell interactions. A: dysmyelinated axons incompletely surrounded by Schwann cell cytoplasm from a My41 mouse. B: abnormal Schwann cell cytoplasmic projections seen in this case in an My41 mouse. C: a demyelinated fibre from the sural nerve of a CMT1A duplication patient.

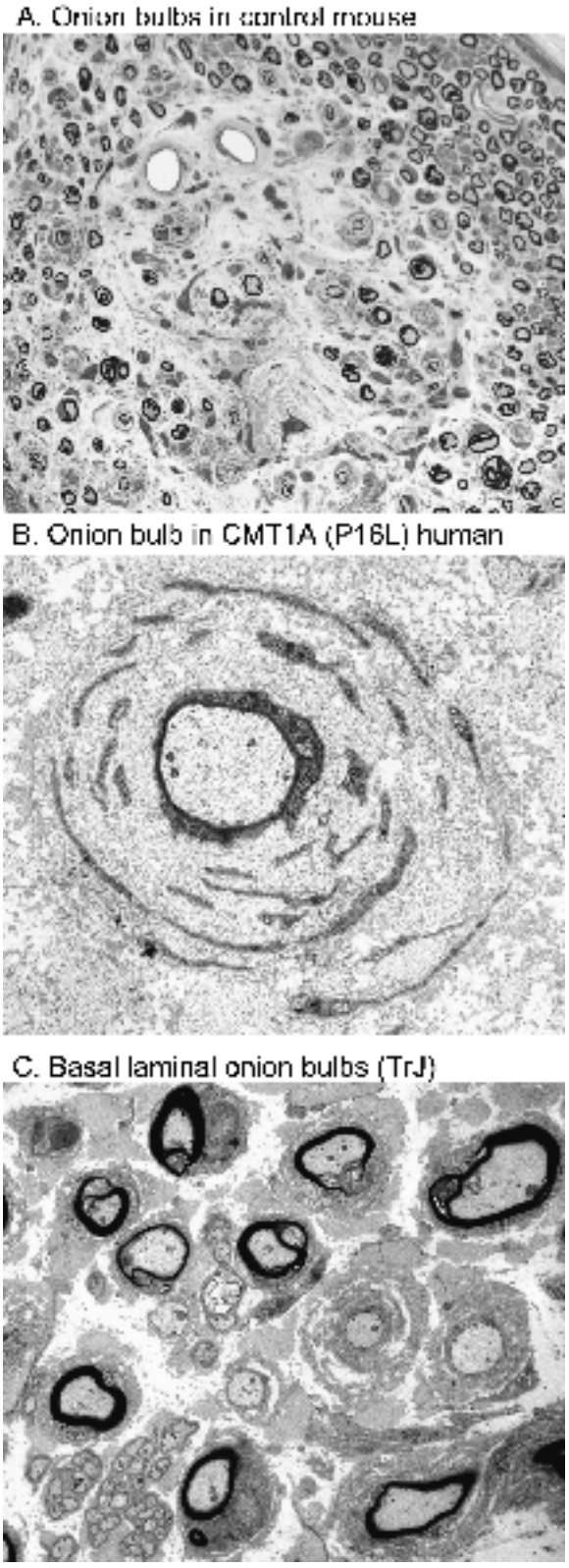

Fig. 9 Onion bulb formations. A: onion bulbs seen in nerve taken from the ankle level of an 18-month-old control mouse. B: a classical onion bulb from a CMT1A (P16L) patient. C: basal laminal onion bulbs from a Tr^J mouse.

over-express PMP22 (Sancho et al. 1999), PMP22 null mutants (Sancho et al. 1999), mice which over-express myelin protein zero (P0) (Wrabetz et al. 2000; Yin et al. 2000) and those in which an epitope tag on P0 results in a gain of function disorder (Previtali et al. 2000).

An increased number of Schwann cells was noted in the first histological descriptions of the Trembler (Tr) mouse (Ayers & Anderson, 1973) and has been found in most PMP22 mutants described since, apart from the very mildly affected C61 strain (Robertson et al. 1999; Sancho et al. 2001). It is a common feature of all types of demyelinated nerve and is not in any sense specific to PMP22 mutant mice. As Schwann cells are known to divide in response to axonal mitogens (Baichwal & DeVries, 1989; Komiyama & Suzuki, 1992), one might expect the number of Schwann cells to correlate with the degree of demyelination. Instead we find the number of Schwann cell nuclei increases to a characteristic level of 12–14 Schwann cell nuclei per 100 axons (about three times normal levels), despite very variable levels of dysmyelination (20% in Tr^J to 75% in My41) (Fig. 3). In tgN248 mice, which have very high mouse *pmp22* expression, there is almost no myelin but they show a similar degree of increase to four times the normal number of Schwann cells (Magyar et al. 1996; Sancho et al. 2001). The same degree of Schwann cell increase is also found in another PMP22 mutant Trembler (G150A) whose nerves have considerably less myelin than Tr^J animals (Sancho et al. 2001). This suggests that there is a maximum possible level of Schwann cells and that this level has already been reached when 20% of axons are dysmyelinated (Tr^J mice). The limited increase in Schwann cell numbers could be due to death of excess cells or a limited proliferative ability. An elevated level of Schwann cell apoptosis has been observed to accompany increased Schwann cell proliferation both in mice deficient in *pmp22* and in the Trembler mouse (Sancho et al. 2001).

In the clinically affected strains we examined (C22, My41 and Tr^J, but not the mild C61 line) myelin sheath thickness is decreased relative to axon size. The g ratios are not, however, increased in proportion to the overall degree of myelin deficit. The measurable myelin sheaths of C22 animals appear to be thinnest (highest g ratio) even though My41 mice have more dysmyelinated fibres (Fig. 3). Myelin sheath periodicity was measured for all the strains but was only significantly increased in C22 mice (Fig. 3). Uncompacted myelin was seen in all models (except C61) but was not specifically

found at either the inner or the outer edge of the myelin sheath.

Sancho et al. (1999) have conducted a detailed study of spinal roots and distal portions of motor and sensory branches of the same nerve. Myelination in the ventral roots of both tgN248 and PMP22$^{0/0}$ null mutant mice was more affected than the dorsal roots. A similar observation was made previously in the Tr^{J} mouse (Robertson et al. 1997) and is also true for C22 and My41 mice (data not shown). This bias towards myelin deficits being greater in motor nerves has been found in many other mouse models with myelin protein alterations (discussed in Sancho et al. 1999). Considerable axon loss was found in the ventral roots of PMP22$^{0/0}$ mice (25%) and also in the quadriceps nerves of both PMP22$^{0/0}$ (40%) and tgN248 (22%) mice at 1 year of age. Electron microscope studies of the tibial nerves of our 18-month C22 and Tr^{J} mutant mice showed fibre atrophy and bands of Büngner indicating recent axonal loss but no regenerative clusters. Counts are currently being performed on these nerves but we found no reduction in fibre number in the sciatic nerves of younger (6–8 month) animals (Fig. 6). Interestingly, in the spinal roots of Tr^{J} mice we found axonal loss only in the dorsal roots of both 3-month and 12-month animals despite the degree of myelination deficit being more severe in the ventral roots (Robertson et al. 1997). Preferential damage of sensory axons has also been indicated in EM studies performed on the spinal roots of C22 and My41 mice in which signs of recent axonal loss were found predominantly in the dorsal roots (data not shown).

In normal mice there are bundles of unmyelinated axons surrounded by a single Schwann cell (Remak fibres). In the over-expression models C22 and My41 (but not the mildly affected C61 strain) these unmyelinated axons show an excess of Schwann cell membrane formation (Fig. 5). These are clearly unmyelinated axons and not promyelinated fibres in an arrested stage of development because they occur in bundles. The unmyelinated fibre bundles of Tr^{J} animals show less excess membrane formation than the over-expressing models but similar formations were also found around collagen pockets, suggesting a Schwann cell recognition problem (Fig. 5D).

The initial stages of myelination were delayed in all the mutants we investigated (except C61). None of the developmental morphometric analyses distinguished any particular type of mutation from the others (Fig. 7).

Most of the abnormal Schwann cell interactions, previously reported in the Tr^{J} mouse (Robertson et al. 1997), were also found in the other models. Failure of correct axon ensheathment and extensive Schwann cell processes were present in My41 and C22 mice (Fig. 8B).

A transgenic mouse line over-expressing mouse *pmp22* has already been produced (Magyar et al. 1996). In this model, tgN248, the magnitude of over-expression, 16 copies of mouse *pmp22,* resulted in a complete failure of myelination. In tgN248 mice the average lifespan exceeded 8 months (Magyar et al. 1996) whereas My41 mice rarely survive longer than 5 months despite having a less severe morphological phenotype. Recent work has demonstrated a macrophage-mediated immune component to a demyelination that primarily results from a genetic abnormality (Schmid et al. 2000; Carenini et al. 2001). P0 mutants (P0+/–) showed an age-related increase in the number of macrophages in the quadriceps nerve that was prevented by crossing them with macrophage-deficient *op/op* mice. Concomitantly, the severity of the demyelination seen in P0+/–, *op/op* mouse nerves was considerably less than that seen in P0+/– mice. The tgN248 mice had no detectable myelin at any age nor did they show any signs of demyelination or remyelination (probably due to a complete failure of myelination). The My41 strain had a degree of myelin formation and there is considerable myelin debris (indicating demyelination) present at all ages. As a lack of myelin *per se* does not appear to compromise survival in the tgN248 mice, it is possible that the shortened life span in My41 mice may be related to a secondary macrophage-mediated immune response to damaged myelin. In addition, Notterpek et al. have recently demonstrated PMP22 immunoreactivity associated with tight junction complexes in rat liver, intestine and cultured epithelial cells (Notterpek et al. 2001). The presence of PMP22 in these other cell types may have a bearing on the aspects of pathology in PMP22 mutant mice that cannot be attributed to myelin dysfunction.

Aside from the variable degree of myelin loss, the type of pathology and its development appear very similar in all the PMP22 mutants that we have examined. This is probably a result of a common pathway being used to deal with any type of myelin protein mutation. The source of the transgene, human in C22 and C61 vs. mouse in My41, did not appear to alter the type of pathology, whereas increased copy number was associated with increased severity.

Pathology in a pmp22 over-expressing rat model

The rat CMT1A model produced by Sereda et al. (1996) shares many pathological features with the mouse models. They have a demyelinating phenotype in which many axons have thin or absent myelin. The myelin abnormality is greater in the ventral roots and motor nerves than it is in their sensory counterparts. Similar to the mouse models it is the large myelinated fibres that appear to be preferentially affected. The rat model produces an abundance of classical onion bulbs by 6 months of age that are not found in the mouse models we have examined and in that sense the rat more closely resembles the human disease. Furthermore, in adult animals both sensory and motor conduction velocities are reduced and EMG abnormalities are found similar to patients. A preliminary study of young animals (3 weeks) shows an early slowing of motor nerve conduction velocities and a marked reduction of the H wave amplitude in front of a normal sensory nerve conduction velocity, suggesting early axonal damage of sensory fibres (Grandis et al. 2001). The degree of axon loss has not yet been examined in this model and it will be interesting to know whether or not the close morphological parallels with human pathology are also reflected in the degree of axon loss.

Comparison of pathology in mouse and human nerve

We have compared peripheral nerve pathology in mice and humans over-expressing PMP22 and with the same P16L mutation. The human and mouse peripheral nervous systems react quite differently to the same mutations both qualitatively and quantitatively.

Although CMT1A is primarily a demyelinating disorder, the degree of functional disability in patients correlates with the degree of axonal loss (Thomas et al. 1997). CMT1A duplication patients have typically lost 95% of their sural nerve axons by the time they are in the forth decade of life (Thomas et al. 1997). The degree of axonal loss in mice is modest by comparison even though they are severely disabled (My41 mice). It has been postulated that the differing degrees of axonal loss could be due to either the difference in life span between the two species or the lengths of the axons involved.

The maximum life span for a mouse is only around 2 years. It has been suggested that the mouse models of PMP22 disorders would develop the same type of pathology as that seen in humans if they had a similar life span. Longitudinal studies on CMT1A duplication patients have shown that clinical (muscle atrophy) and electrophysiological abnormalities in children are not detectable until they are at least 2 years old (Berciano et al. 2000). In contrast, affected mice can be identified clinically from 3 weeks of age and show pathological abnormalities from postnatal day 4 (C22, My41 and Tr^J) (Fig. 7). Both the C22 and the My41 strains have levels of over-expression that are several times higher than would occur in duplication patients. As a consequence, much of the phenotype results from a developmental failure of myelination (delayed myelination and reduced number of myelinated fibres) and not from repeated cycles of demyelination and remyelination as seen in humans. Similarly, the development of Tr^J mice is delayed and the number of myelinated fibres is reduced from postnatal day 4. From a very early stage the pathology and its development in these strains was different to that seen in humans and we consider it unlikely that these mouse models would ever develop a phenotype similar to that seen in human disease even after an extended time period. The C61 strain has lower expression and a very mild demyelinating phenotype, as opposed to delayed myelination (Robertson et al. 1999). Mice up to 18 months old show no evidence of developing the features of human disease (axonal loss and onion bulbs) but we cannot say that they would never do so.

In all the mouse models we have examined there was a distinct population of dysmyelinated axons that appeared healthy despite the absence of myelin. A proportion of these axons were not even completely surrounded by Schwann cell cytoplasm. In contrast, demyelinated axons in the nerves of both duplication and P16L patients were only rarely found and they had a normal relationship with the Schwann cells (Fig. 8C). It is possible that the smaller dimensions of mouse axons allows them to remain viable without normal Schwann cell support.

Both human and mouse models show a clear increase in the number of Schwann cells. However, their spatial arrangement is quite different. In both mice and humans with the P16L mutation there is a similar increase of about three- to four-fold in the number of Schwann cells that are attached to axons. In humans, however, there is an additional population of Schwann cells that are not attached to an axon but remain supernumary, usually associated with onion bulbs, giving

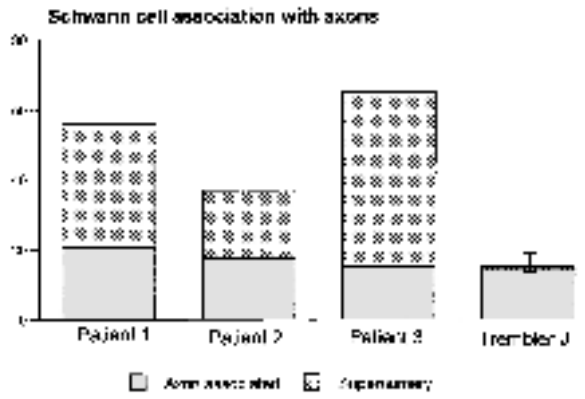

Fig. 10 Schwann cell association with axons in humans and mice with the P16L mutation. Number of Schwann cell nuclei per 100 axons in three patients and six Tr^{J} mice.

a total increase of about 10-fold (Fig. 10). The data presented here are from P16L patients and Tr^{J} mice but similar patterns were also seen in duplication patients and over-expressing mice. The onion bulbs that are a striking feature of both over-expressing and point mutation CMT1A nerve are formed by circular arrangements of excess Schwann cell processes around the central fibres (Fig. 9B). These Schwann cells are generally considered to have resulted from previous cycles of demyelination and remyelination. Onion bulbs are found associated with practically all myelinated fibres in P16L patients and most fibres in duplication patients (Gabreëls-Festen et al. 1995). None of the mouse models we examined had the extensive onion bulb formations seen in humans although mouse Schwann cells in other situations are capable of producing them (Ohara & Ikuta, 1988). In caged rodents, local trauma in the feet induces demyelination and degeneration (Fullerton & Gilliatt, 1967; Thomas et al. 1980) and this probably explains the onion bulbs seen in one of our control mice (Fig. 9A). In contrast, the PMP22 transgenic or mutant murine models had basal laminal onion bulbs with few Schwann cell processes (Fig. 9C). A major difference between the human and mouse models is the presence in CMT1A patients of axonal regeneration. This produces regenerative clusters in the centre of some onion bulbs and may be the source of the myelinated and unmyelinated fibres seen in the peripheral layers of Schwann cells. An alternative source for these axons is colateral sprouting at the nodes of Ranvier. It is probably the presence of these axons that converts the redundant Schwann cells into a permanent or semipermanent feature. The absence of regenerating or colateral sprouts in the mouse may explain why extensions and reduplication of Schwann cell processes are short-lived. It is interesting to note that in a rat model with over-expression of mouse pmp22, onion bulbs are present in older animals (Sereda et al. 1996). Colateral sprouting has been found in other models of demyelination in the rat (McDonald, 1963). These may be related to the spiky processes that may be seen at the nodes of Ranvier in rat nerves. These are not a feature of mouse nerves. This again demonstrates the species specificity of Schwann cell response to the same mutation.

The unmyelinated fibre bundles (Remak fibres) in mouse mutant and over-expressing models have multiple layers of Schwann cell cytoplasm around the axons (Fig. 5). In humans, it is more difficult to identify Remak fibres as they contain only one or two axons and are easily confused with axonal sprouts. However, in the over-expressing and P16L humans we could find no evidence of any Schwann cell abnormality associated with unmyelinated fibres.

In an interesting experiment, Sahenk and colleagues took sural nerve segments from CMT1A (over-expressing) patients and grafted them in to the sciatic nerves of nude mice (Sahenk et al. 1999). As the mouse axons regenerated through the graft they were ensheathed and myelinated by human Schwann cells. In the distal region of the graft, human Schwann cells began to produce CMT1A-like features that are not normally seen even in transgenic models that over-express the human or mouse PMP22 protein. These included classical onion bulb formation, axon degeneration and axon loss. This suggests that human-derived Schwann cells respond fundamentally differently to the murine ones even when they are over-expressing the same protein and that they in turn affect axons differently.

Summary

The murine mutants that we examined all had essentially the same type of pathology. The dominant features were myelin deficit, Schwann cell proliferation and developmental delays in myelination. Qualitatively, the mouse models showed similar abnormal Schwann cell interactions with both myelinated and unmyelinated fibre populations. We conclude that the phenotypes produced by over-expressing and missense mutations probably result from a common pathway being used to deal with both types of pmp22 abnormality.

The murine and human peripheral nervous systems react very differently to the same PMP22 mutation and to over-expression. Mutant mice have considerably less axonal loss than humans and a population of dysmyelinated fibres. Demyelinated axons in the mouse often have very little or no Schwann cell contact whereas in humans demyelinated axons appear to have a normal relationship with Schwann cells. Unmyelinated (Remak) fibres in humans appear normal whereas in mutant mice Schwann cells produce spirals of cytoplasm reminiscent of uncompacted myelin. The relationship of Schwann cells with their axons differs in humans where most Schwann cells are supernumary to the axon associated with onion bulbs, whereas in mice they are almost exclusively axon associated and only basal laminal onion bulbs are seen.

Acknowledgments

This work was supported by grants from Action Research and the Wellcome Trust.

References

Ayers MM, Anderson RM (1973) Onion bulb neuropathy in the Trembler mouse: a model of hypertrohic interstitial neuropathy (Dejerine-Sottas) in man. *Acta*. *Neuropathol*. **25**, 54–70.

Baichwal RR, DeVries GH (1989) A mitogen for Schwann cells derived from myelin basic protein. *Biochem*. *Biophys*. *Res*. *Comm*. **164**, 883–888.

Berciano J, Garcia A, Calleja J, Combarros O (2000) Clinico-electrophysiological correlation of extensor digitorum brevis muscle atrophy in children with Charcot-Marie-Tooth disease 1A duplication. *Neuromusc*. *Disord*. **10**, 419–424.

Carenini S, Maurer M, Werner A, Blazyca H, Toyka KV, Schmid CD, et al. (2001) The role of macrophages in demyelinating peripheral nervous system of mice heterozygously deficient in pO. *J*. *Cell*. *Biol*. **152**, 301–308.

Fullerton PM, Gilliatt RW (1967) Pressure neuropathy in the hind foot of the guinea pig. *J*. *Neurol*. *Neurosurg*. *Psychiatry* **30**, 18–25.

Gabreëls-Festen AAWM, Bolhuis PA, Hoogendijk JE, Valentijn LJ, Eshuis EJHM, Gabreëls FJM (1995) Charcot-Marie-Tooth disease type IA: morphological phenotype of the 17p duplication versus PMP22 point mutations. *Acta Neuropathol*. **90**, 645–649.

Gnirke A, Huxley C, Peterson K, Olson MV (1993) Microinjection of intact 200- to 500-kb fragments of YAC DNA into mammalian cells. *Genomics* **15**, 659–667.

Grandis M, Abbruzzese M, Mancardi G, Leandri M, Nobbio L, Schenone A (2001) Early electrophysiological chagnes in a transgenic rat model of Charcot-Marie-Tooth. *J*. *Peripheral Nervous System* Abstract 6, 143.

Haldi ML, Strickland C, Lim P, VanBerkel V, Chen X-N, Noya D, et al. (1996) A comprehensive large-insert yeast artificial chromosome library for physical mapping of the mouse genome. *Mamm*. *Genome* **7**, 767–769.

Hogan B, Costantini F, Lacy E (1986) *Manipulating the Mouse Embryo*. Cold Spring Harbor Press.

Huxley C, Passage E, Robertson AM, Youl B, Huston S, Manson A, et al. (1998) Correlation between varying levels of PMP22 expression and the degree of demyelination and reduction in nerve conduction velocity in transgenic mice. *Hum*. *Mol*. *Genet*. **7**, 449–458.

Komiyama A, Suzuki K (1992) Age-related differences in proliferative responses of Schwann cells during Wallerian degeneration. *Brain Res*. **573**, 267–275.

Lewis BC, Shah NP, Braun BS, Denny CT (1992) Creation of a yeast artificial chromosome fragmentation vector based on lysine-2. *Genet*. *Anal*. *Techn Appl*. **9**, 86–90.

Lupski JR, Montes de Oca-Luna R, Slaugenhaupt S, Pentao L, Guzzetta V, Trask BJ, et al. (1991) DNA duplication associated with Charcot-Marie-Tooth disease type 1A. *Cell* **66**, 219–232.

Magyar JP, Martini R, Ruelicke T, Aguzzi A, Adlkofer K, Dembic Z, et al. (1996) Impaired differentiation of Schwann cells in transgenic mice with increased PMP22 gene dosage. *J*. *Neurosci*. **16**, 5351–5360.

McDonald WI (1963) The effects of experimental demyelination on conduction in peripheral nerve: a histological and electrophysiological study. 1. Clinical and histological observations. *Brain* **86**, 481–500.

Nelis E, Van Broeckhoven C, De Jonghe P, Lofgren A, Vandenberghe A, Latour P, et al. (1996) Estimation of the mutation frequencies in Charcot-Marie-Tooth disease type 1 and hereditary neuropathy with liability to pressure palsies: a European collaborative study. *Eur*. *J*. *Hum*. *Genet*. **4**, 25–33.

Notterpek L, Roux KJ, Amici SA, Yazdanpour A, Rahner C, Fletcher BS (2001) Peripheral myelin protein 22 is a constituent of intercellular junctions in epithelia. *Proc*. *Natl Acad*. *Sci*. *USA* **98**, 14404–14409.

Ohara S, Ikuta F (1988) Schwann cell responses during regeneration after one or more crush injuries to myelinated nerve fibres. *Neuropathol*. *Appl*. *Neurobiol*. **14**, 229–245.

Pentao L, Wise CA, Chinault AC, Patel PI, Lupski JR (1992) Charcot-Marie-Tooth type 1A duplication apears to arise from recombination at repeat sequences flanking the 1.5 Mb monomer unit. *Nat*. *Genet*. **2**, 292–300.

Previtali S, Quattrini A, Fasolini M, Panzeri MC, Villa A, Filbin MT, et al. (2000) Epitope-tagged Po glycoprotein causes Charcot-Marie-Tooth-like neuropathy in transgenic mice. *J*. *Cell*. *Biol*. **151**, 1035–1045.

Raeymaekers P, Timmerman V, Nelis E, De Jonghe P, Hoogendijk JE, Baas F, et al. (1991) Duplication in chromosome 17p11.2 in Charcot-Marie-Tooth neuropathy type 1a (CMT 1a). The HMSN Collaborative Research Group. *Neuromusc*. *Disord*. **1**, 93–97.

Reilly M (1998) Genetically determined neuropathies. *J*. *Neurol*. **245**, 6–13.

Robertson AM, Huxley C, King RHM, Thomas PK (1999) Development of early postnatal peripheral nerve abnormalities in Trembler-J and PMP22 transgenic mice. *J*. *Anat*. **195**, 331–339.

Robertson AM, King RHM, Muddle JR, Thomas PK (1997) Abnormal Schwann cell/axon interactions in the Trembler-J mouse. *J. Anat.* **190**, 423–432.

Sahenk Z, Chen L, Mendell JR (1999) Effects of PMP22 duplication and deletions on the axonal cytoskeleton. *Ann. Neurol.* **45**, 16–24.

Sancho S, Magyar JP, Aguzzi A, Suter U (1999) Distal axonopathy in peripheral nerves of *PMP22* -mutant mice. *Brain* **122**, 1563–1577.

Sancho S, Young P, Suter U (2001) Regulation of Schwann cell proliferation and apoptosis in PMP22-deficient mice and mouse models of Charcot-Marie-Tooth disease type 1A. *Brain* **2001**, 2177–2187.

Schmid CD, Stienekemeier M, Oehen S, Bootz F, Zielasek J, Gold R, et al. (2000) Immune deficiency in mouse models for inherited peripheral neuropathies leads to improved myelin maintenance. *J. Neurosci.* **20**, 729–735.

Sereda M, Griffiths IP, Pühlhofer A, Stewart H, Rossner MJ, Zimmermann F, et al. (1996) A transgenic rat model of Charcot-Marie-Tooth Disease. *Neuron* **16**, 1049–1060.

Thomas PK, King RHM, Sharma AK (1980) Changes with age in the peripheral nerves of the rat. *Acta. Neuropathol. (Berl)* **52**, 1–6.

Thomas PK, Marques WJ, Davis MB, Sweeney MG, King RHM, Bradley JL, et al. (1997) The phenotypic manifestations of chromosome 17p11.2 duplication. *Brain* **120**, 465–478.

Wise CA, Garcia CA, Davis SN, Heju Z, Pentao L, Patel PI, et al. (1993) Molecular Analyses of unrelated Charcot-Marie-Tooth (CMT) disease patients suggest a high frequency of the CMT1A duplication. *Am. J. Hum. Genet.* **53**, 853–863.

Wrabetz L, Feltri ML, Quattrini A, Imperiale D, Previtali S, D'Antonio M, et al. (2000) Po overexpression causes congenital hypomyelination of peripheral nerves. *J. Cell. Biol.* **148**, 1021–1033.

Yin X, Kidd GJ, Wrabetz L, Feltri ML, Messing A, Trapp BD (2000) Schwann cell myelination requires timely and precise targeting of Po protein. *J. Cell. Biol.* **148**, 1009–1020.